

Supplementary Materials for

H₂S-Induced Sulfhydrylation of the Phosphatase PTP1B and Its Role in the Endoplasmic Reticulum Stress Response

Navasona Krishnan, Cexiong Fu, Darryl J. Pappin, Nicholas K. Tonks*

*To whom correspondence should be addressed. E-mail: tonks@cshl.edu

Published 13 December 2011, *Sci. Signal.* **4**, ra86 (2011)
DOI: 10.1126/scisignal.2002329

The PDF file includes:

- Fig. S1. Time-dependent inactivation of PTP1B by H₂O₂.
- Fig. S2. Time-dependent inactivation of PTP1B by NO.
- Fig. S3. Time-dependent reactivation of PTP1B by TR/TRR.
- Fig. S4. Time-dependent reactivation of PTP1B by GSH.
- Fig. S5. Mechanism of PTP labeling by the IAP probe.
- Fig. S6. Induction of ER stress by tunicamycin.
- Fig. S7. Decrease in CSE by RNAi.
- Fig. S8. Changes in components of the UPR after exposure to thapsigargin.
- Fig. S9. Proposed mechanism for persulfide modification of PTP1B.
- Table S1. Quantitation of the different redox forms of Cys²¹⁵ in PTP1B observed after induction of ER stress with tunicamycin.

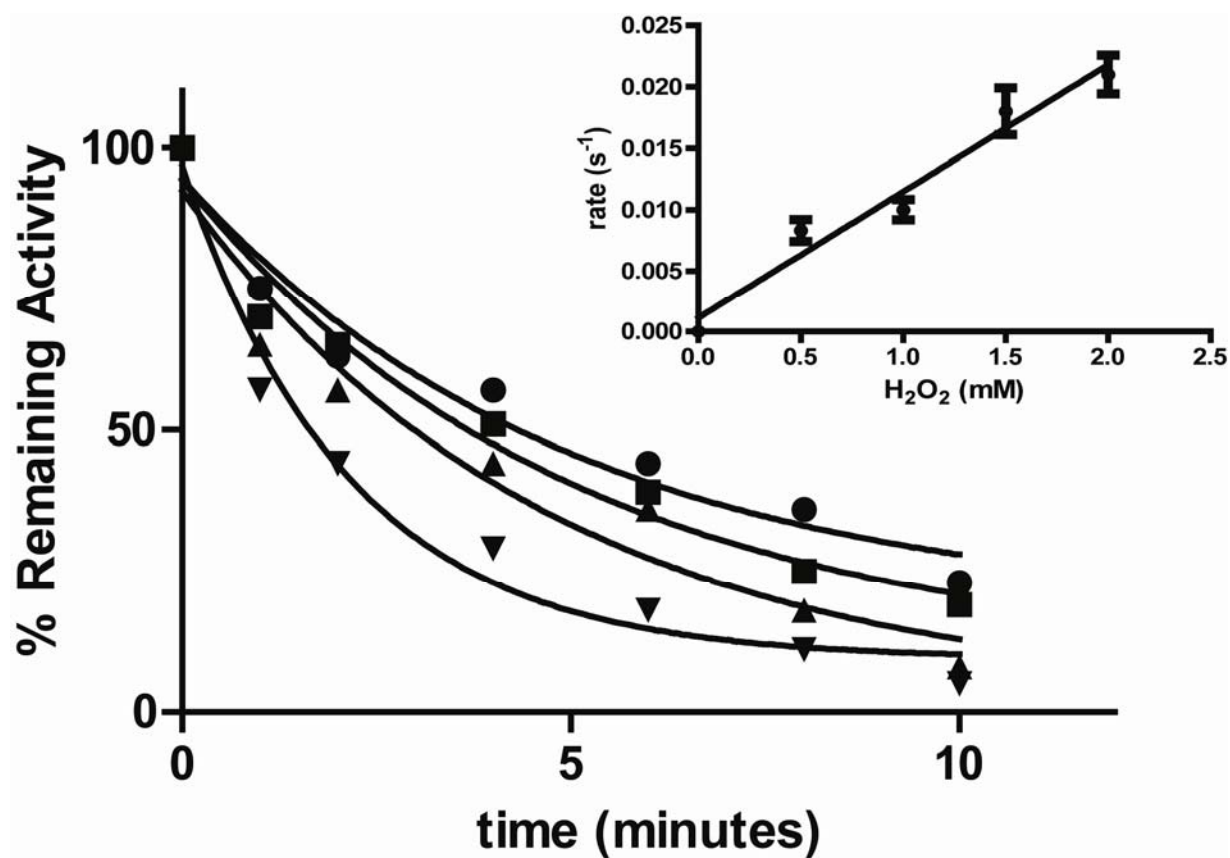


Figure S1. Time-dependent inactivation of PTP1B by H₂O₂. The phosphatase activity of PTP1B was monitored in the presence of H₂O₂, 0.5 mM (●), 1 mM (■), 1.5 mM (▲), 2 mM (▼). Inset, the concentration dependence of the rate of inactivation was used to derive the second order rate constant, $10 \pm 1.4 \text{ M}^{-1}\text{s}^{-1}$. Data are derived from three independent determinations.

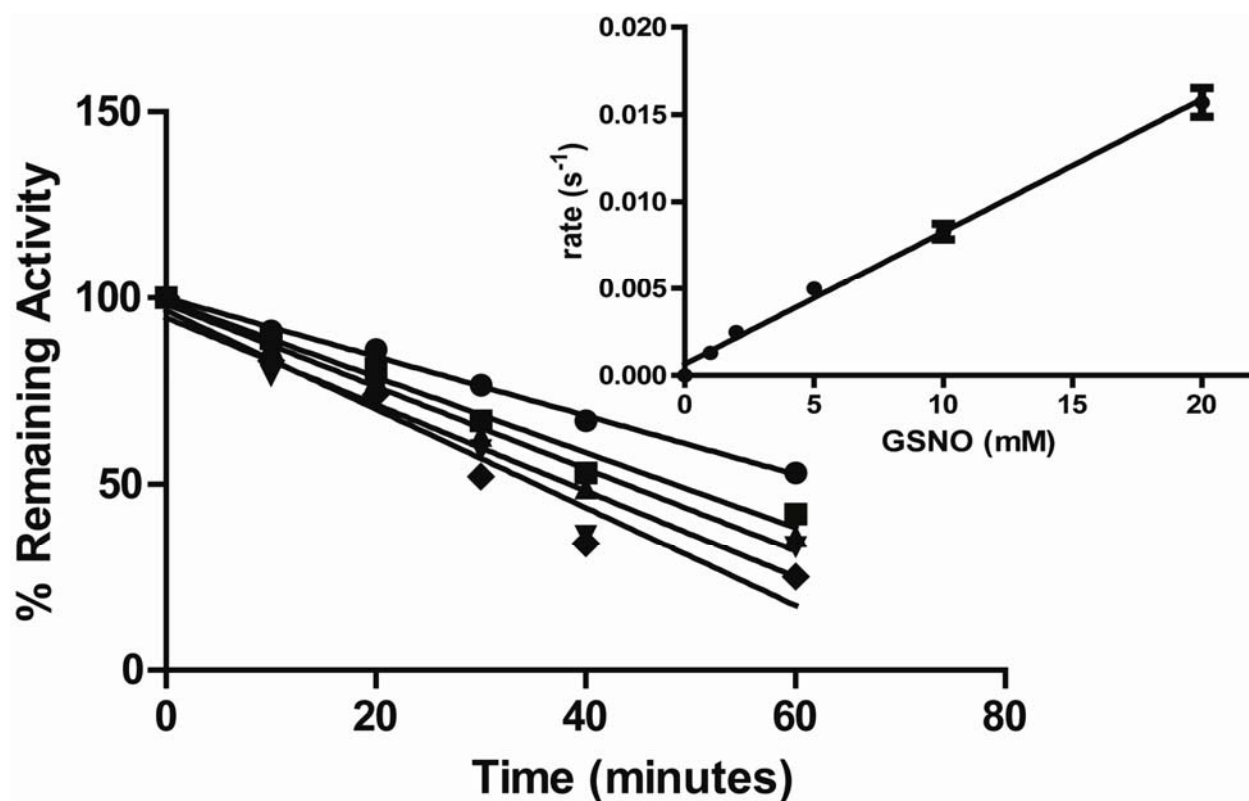


Figure S2. Time-dependent inactivation of PTP1B by NO. The phosphatase activity of PTP1B was monitored in the presence of GSNO, 1 mM (●), 2 mM (■), 5 mM (▲), 10 mM (▼), 20 mM (◆). Inset, the concentration dependence of the rate of inactivation was used to derive the second order rate constant, $2.1 \pm 0.5 \text{ M}^{-1}\text{s}^{-1}$. Data are derived from three independent determinations.

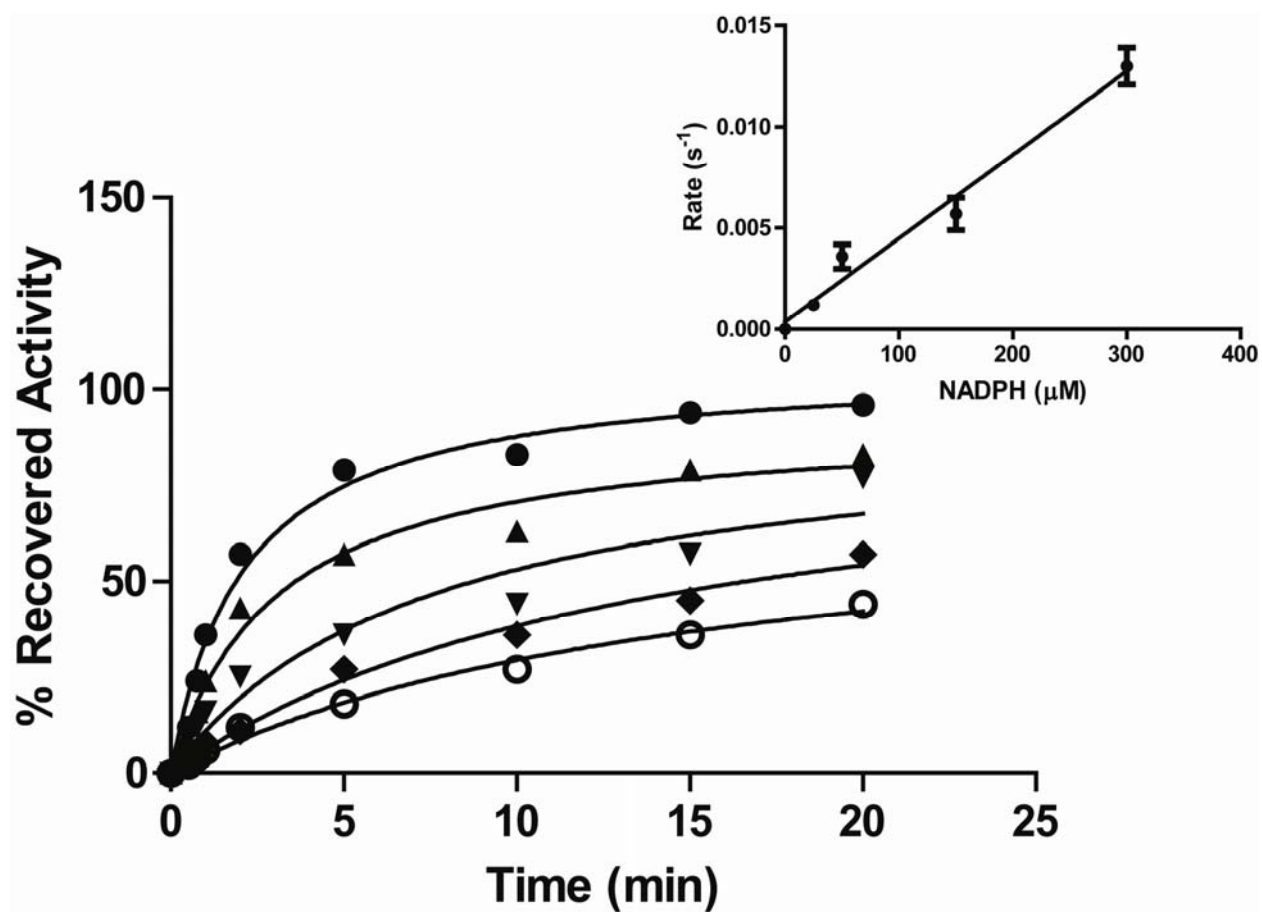


Figure S3. Time-dependent reactivation of PTP1B by TR/TRR. NADPH was used at 10 μM (o), 25 μM (♦), 50 μM (▼), 150 μM (▲) or 300 μM (●). Inset: the second order rate constant, $45.5 \pm 2.8 \text{ M}^{-1}\text{s}^{-1}$, was derived from the concentration dependence of the rate of inactivation. Data are derived from three independent determinations.

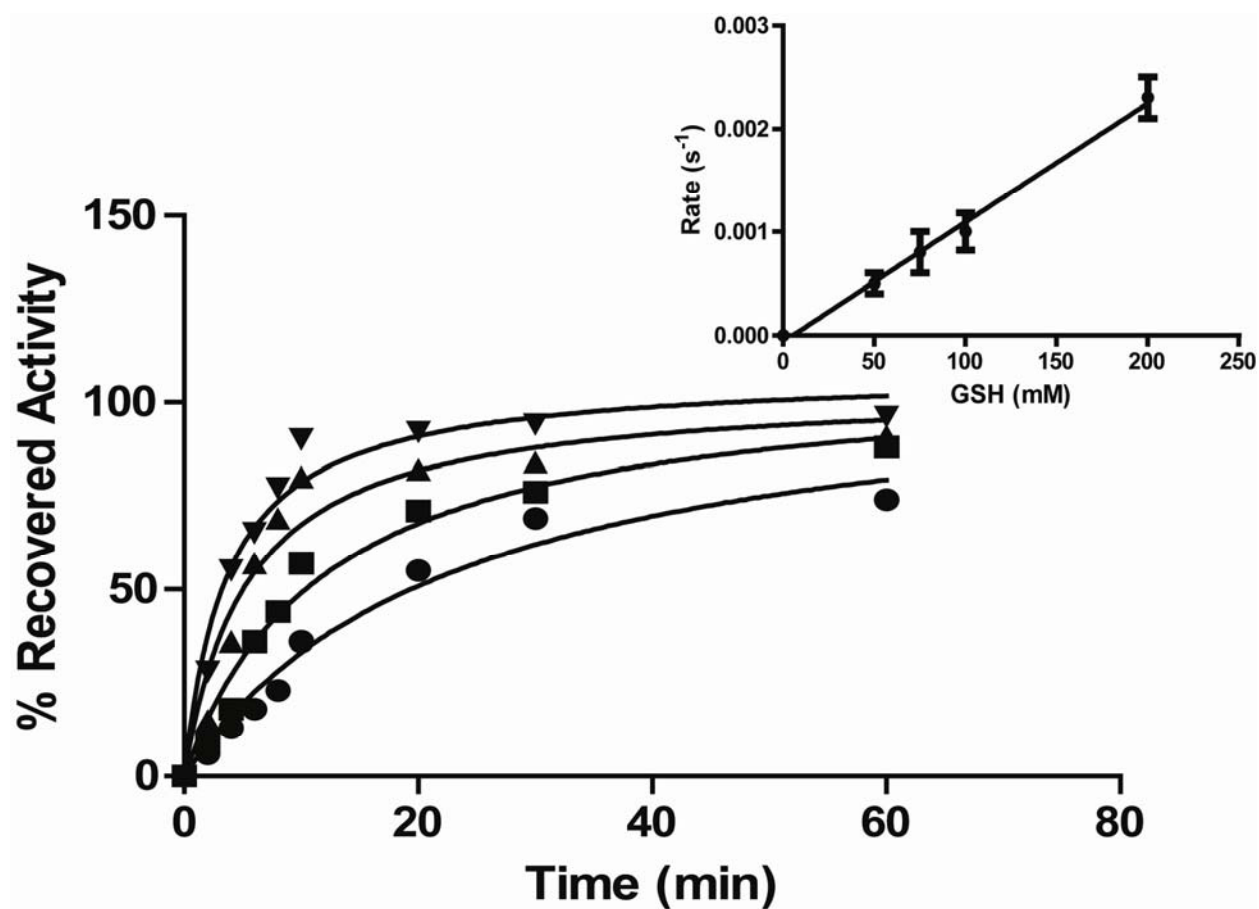


Figure S4. Time-dependent reactivation of PTP1B by GSH. GSH was used at 50 mM (●), 75 mM (■), 100 mM (▲), or 200 (▼) mM. Inset: the second order rate constant, $0.013 \pm 0.012 \text{ M}^{-1}\text{s}^{-1}$, was derived from the concentration dependence of the rate of inactivation. Data are derived from three independent determinations.

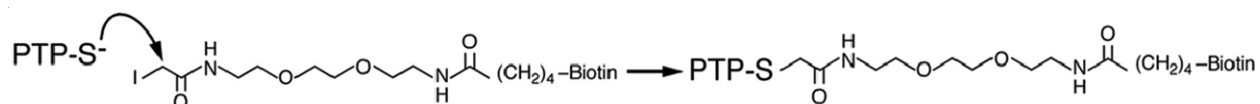


Figure S5. Mechanism of PTP labeling by the IAP probe. Schematic mechanism of PTP reactivity towards a biotinylated iodoacetyl-polyethylene glycol(IAP) probe. Adapted from Boivin, B., *et al.*, A modified cysteinyl-labeling assay reveals reversible oxidation of protein tyrosine phosphatases in angiomyolipoma cells. *Proc. Natl. Acad. of Sci. U. S. A.* **105**, 9959-9964 (2008).]

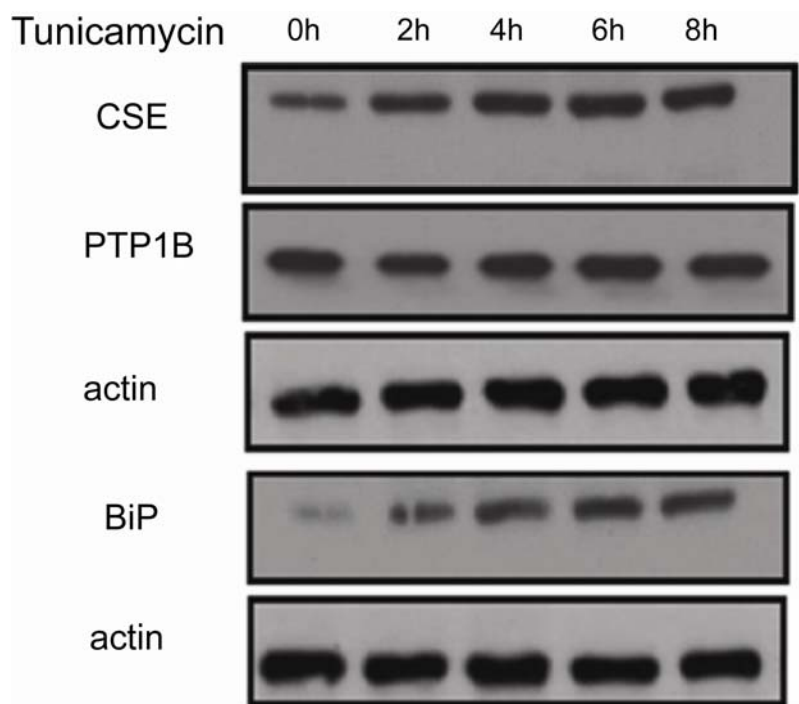


Figure S6. Induction of ER stress by tunicamycin. Representative immunoblots of cystathionine- γ -lyase (CSE), PTP1B, and the ER chaperone BiP from cell lysates following exposure to tunicamycin (10 μ g/ml) for 0, 2, 4, 6, or 8 hours. Actin served as the loading control. Data are representative of three independent experiments.

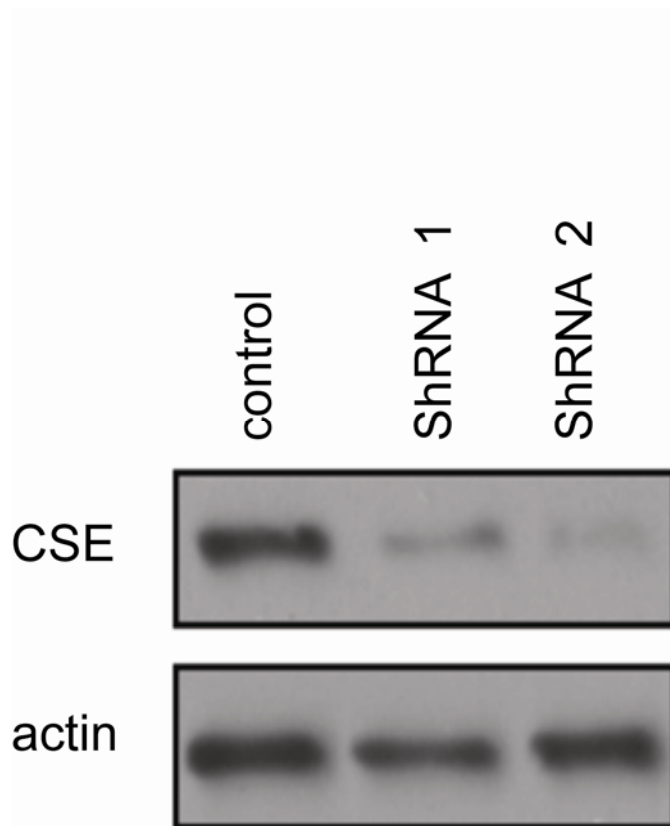


Figure S7. Decrease in CSE by RNAi. Representative immunoblot to show the abundance of CSE) in cells expressing specific shRNAs (shRNA1 and shRNA2) compared to control luciferase shRNA-expressing cells. Actin served as the loading control. Data are representative of three independent experiments.

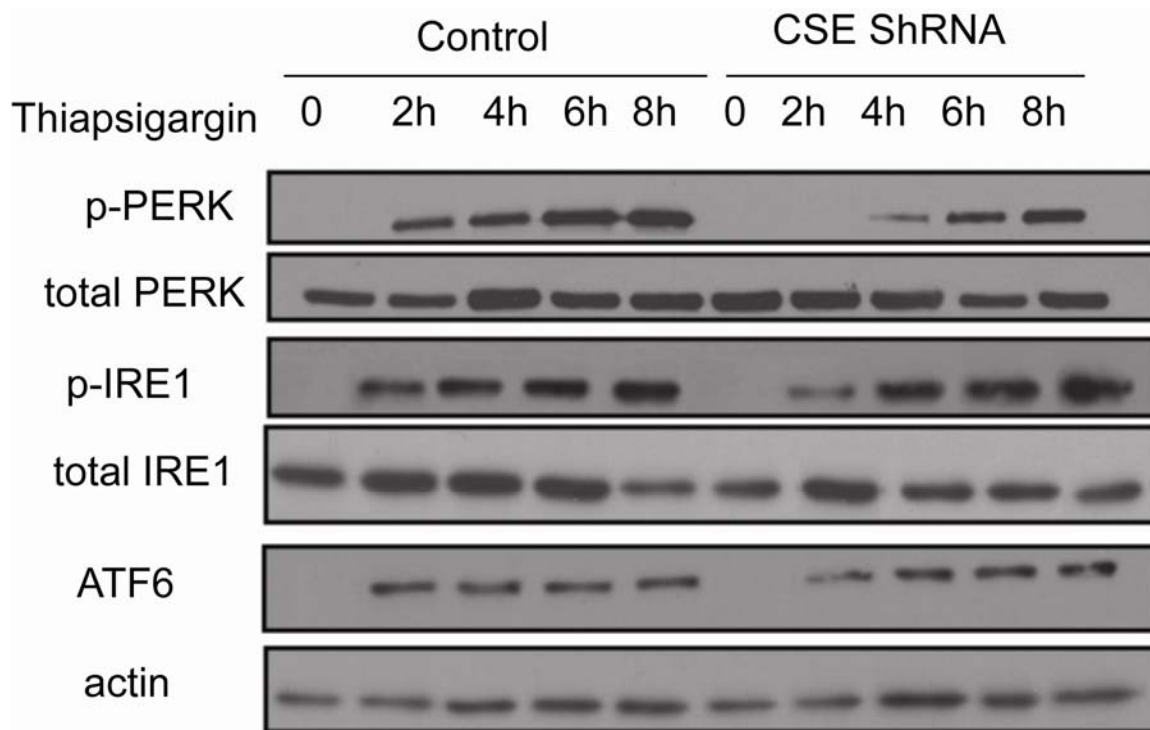


Figure S8. Changes in components of the UPR after exposure to thapsigargin. ER stress was induced by thapsigargin (TG, 1 μ M) for 0, 2, 4, 6, or 8 hours. Immunoblot showing activation of components of the UPR. The data illustrate a time course, over 0-8 h, to examine activation of PERK [anti-phospho-PERK (Thr980) compared to total PERK (anti-PERK)], and the activation of IRE1 [anti-phospho-IRE1 α (Ser724) compared to total IRE1 (anti-IRE1 α)] in control and CSE-deficient cells. There was no obvious difference in the abundance of ATF6. Data are representative of three independent experiments.

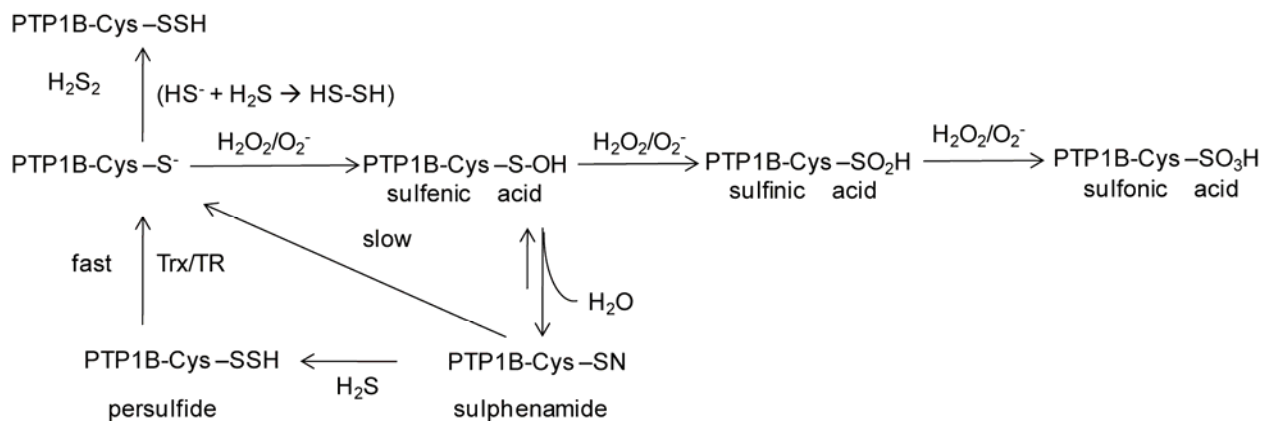


Figure S9. Proposed mechanism for persulfide modification of PTP1B. The thiolate anion (Cys²¹⁵) in the active site of PTP1B is highly susceptible to oxidation. Upon oxidation, it forms a stable cyclic sulphenamide intermediate, which has been postulated to promote reversibility of oxidation. Higher oxidation, to sulfenic and sulfonic acid, generates irreversibly oxidized forms of PTP1B. Reaction of H₂S with the cyclic sulphenamide would be expected to generate the persulfide modification that we detected, which could protect PTP1B from higher irreversible oxidation and may also promote reactivation through thioredoxin. Alternatively H₂S could also form a persulfide on reaction with hydrogen peroxide, which could react directly with reduced PTP1B.

Time (h)	control (%)				CSE ShRNA (%)			
	-SH	-SSH	-SO ₂ H	-SO ₃ H	-SH	-SSH	-SO ₂ H	-SO ₃ H
0	95	3.5	0.8	0.7	94	4.8	5	0.4
2	94	3.2	2.5	0.3	83	7.9	8.3	8.6
4	53.5	38	3.2	3.4	80	8.2	11	11.3
6	50	42.2	2.9	4.1	80	8.4	15	10.9
8	50	43.1	3.6	0.4	79	10.8	12	7.5

Table S1. Quantitation of the different redox forms of Cys²¹⁵ in PTP1B observed after induction of ER stress with tunicamycin. Control and CSE depleted Hela cells were exposed to tunicamycin for 0, 2, 4, 6, and 8 hours following which immunopurified PTP1B was analyzed by mass spectrometry. Data are representative of three experiments.